Boosting the guerbet reaction: A cooperative catalytic system for the efficient bio-ethanol refinery to second-generation biofuels

Boosting the Guerbet Reaction: a cooperative catalytic system for the efficient bio-ethanol refinery to second-generation biofuels.

Cristiana Cesari,[a*] Anna Gagliardi,[a] Alessandro Messori,[a] Nicola Monti,[a] Valerio Zanotti,[a,b] Stefano Zacchini,[a] Ivan Rivalta,[a,c] Francesco Calcagno,[a] Carlo Lucarelli,[d] Tommaso Tabanelli,[a,b] Fabrizio Cavani[a,b] and Rita Mazzoni,[a,b*]

[a]Department of Industrial Chemistry "Toso Montanari", viale Risorgimento, 4 40136 Bologna. [b]Interdepartmental Centre for Industrial Research, Renewable Sources Environment, Sea, Energy (CIRI-FRAME), viale Risorgimento, 4 40136 Bologna, Italy. [c]University of Lyon, École Normale Supérieure de Lyon, CNRS UMR 5182, Laboratoire de Chimie, 46 allée d'Italie, F69364 Lyon, France. [d]Department of Science and High Technology, via Valleggio, 9, 22100 Como.

Corresponding author: * **Rita Mazzoni** e-mail: rita.mazzoni@unibo.it; * **Cristiana Cesari** e-mail: cristiana.cesari2@unibo.it.

Abstract

The catalytic activity of anionic ruthenium complexes toward the transformation of bio-ethanol to 1-butanol and higher alcohols is found to be dependent on the imidazolium counterion. After the identification of a parallel reaction involving the catalyst in hydrogen evolution, conversion and selectivity are impressively boosted by the addition of p-benzoquinones as co-catalysts. The catalytic system avoids the side reaction and led to highly competitive conversions up to 88% (0.2% mol ruthenium catalyst loading, 1.5% mol benzoquinone loading). Butanol and higher alcohols are produced in yields up to 85% (overall selectivity 97%) as a mixture of valuable alcohols for advanced biofuel and lubricants applications. The catalytic system can be recycled and the reaction

shows comparable efficiency on a real matrix (alcohol from wine production chain wastes) even in the presence of significant amounts of water, thus closing a hypothetic economic circle. A reaction mechanism is proposed for the most promising ruthenium complex working in cooperation with the most efficient co-catalyst: p-benzoquinone.

Keywords

Bio-ethanol; bio-refinery; ruthenium molecular catalysts; benzoquinone; imidazolium salts.

1. Introduction

The global community has acknowledged biofuel for providing sustainable energy, thereby reducing the dependence on fossil fuels. Bio-ethanol refinery is thus conceived to develop new economic strategies for upgrading the fuel properties of this bio-derived platform chemical into species with higher energy density and greater miscibility with conventional fuel.[1-6] In terms of energy density, linear alcohols are very close to gasoline and can be employed in fuel blends for diesel engines (with a formulation of up to 30% of alcohols in diesel fuel).[7] However, drawbacks can arise due to their poor lubricant properties that can negatively influence an engine's durability.[8] To overcome this problem, mixtures also containing branched alcohols are already used as lubricants (in particular 2-alkyl alcohols, also known as Guerbet alcohols).[9] An industrial scale-up of second-generation biofuels-production processes from waste-derived feedstocks is, however, still hampered by several critical technological issues and bottleneck steps. An attractive route for the catalytic conversion of bio-ethanol into butanol and higher alcohols (both linear and branched) is the Guerbet reaction, which in theory furnishes an ideal mechanism for alcohol homologation.[1-6] While simple in principle, this is difficult in application due to several concerns encountered in increasing selectivity and conversion.

One of the main troubles of this process resides in the aldol condensation of acetaldehyde, which is catalyzed by a base. This reaction can, in fact, further evolve towards the formation of undesired insoluble invaluable polymers.[10-16]

Looking for a route to solve these drawbacks, in 2016, after their pioneering work with ruthenium phosphine catalysts,[17] Wass et al. coined the idea of "Guerbet renewed" from a new perspective: homogeneous catalysis.[18] Indeed, homogeneous approaches for ethanol homologation to 1-butanol and higher alcohols employ iridium, ruthenium and manganese bifunctional catalysts which require milder reaction conditions and showed a larger control on yields and selectivity in comparison to heterogeneous catalysis. [19-23] First drawbacks for the still most efficient ruthenium complexes were highlighted by Wass et al. in 2013[17] and confirmed by Szymczak group[24] as the inverse correlation between butanol yield and selectivity. With a tandem catalytic approach involving iridium, copper or nickel complexes, Jones and co-workers were later able to keep a 99% butanol selectivity up to 37% yield.[25] At the same time, by employing a ruthenium catalyst with a tridentate ligand, Milstein group extended the homogeneous Guerbet reaction concept to the co-valorization of higher alcohols, such as hexanol C_6 and octanol C_8.[26] The current interest in this reaction and its drawbacks have also been nicely documented by Liauw and co-workers, who deeply analyzed the reason for the failure in alcohol homologation of a good candidate such as the bifunctional catalyst Ru-MACHO-BH.[27] Exploring real matrix derived feedstocks, Wass and co-workers lately demonstrated some water tolerance in a nice transformation of fermentation broths (first-generation biomass) into iso-butanol.[28] Furthermore, we recently reported a phosphine-free ionic ruthenium cyclopentadienone complex for the production of second-generation biofuels from wine waste derived bio-ethanol.[29] Although the reaction would well fit in a contest of circular economy in the wine production chain, LCA (life cycle assessment) and engineering assessments suggested that the process needs to be improved in terms of efficiency to become suitable for industrial application. With this aim in mind, our focus is here devoted to

deepen the reactivity of anionic ruthenium complexes by changing the counterion, thus investigating the role of the imidazolium salts. While trying to solve this latter problem by implementing the catalytic system with a benzoquinone as a co-catalyst, an impressive boost in conversion and alcohol yields was obtained. The new system reaches the most promising performances in terms of EtOH conversion and alcohols yield reported so far.

2. Experimental section

2.1 Materials

Diethyl ether (Et_2O), tetrahydrofuran (THF), acetonitrile (CH_3CN), dichloromethane (CH_2Cl_2), and hexane were distilled before use and stored in Schlenk flasks containing pre-dried molecular sieves. Ethylacetate (EtOAc), chloroform, ethanol (EtOH), iso-propanol (^{i}PrOH), heptane, toluene, $CDCl_3$, D_2O, acetone-d_6, toluene-d_8 (VWR) and other solvents not previously listed were used without additional purification.

Triruthenium-dodecacarbonyl ($Ru_3(CO)_{12}$) (Stream), silver oxide, methyl iodide, 1-methylimidazole, tetraethylammonium iodide, paraformaldehyde, 1,3 diphenylacetone, tert-butylamine, acetic acid, glyoxal, sodium methoxide (NaOMe), sodium hydroxide (NaOH) (Sigma Aldrich), sodium ethoxide (NaOEt), 4,4'dimethoxybenzil, 1,2-dimethylimidazole, 2,6-diisopropylaniline, 2,6-dimethoxy-1,4-benzoquinone (BQ-OMe) (Alfa Aesar), were used as purchased. 1,3-dimethylimidazolium iodide (**1a**), 1,2,3-trimethylimidazolium iodide (**1b**), 1,3-bis(2,6-diisopropylphenyl)imidazolium chloride (**1c**), 3,4-bis(4-methoxyphenyl)-2,5-diphenylcyclopenta-2,4-dienone, dicarbonyl(η4-3,4-bis(4-methoxyphenyl)-2,5-diphenylcyclopenta-2,4-dienone) ruthenium dimer (**2**), were prepared as previously reported.[29, 30] p-benzoquinone (Alfa Aesar) was purified by column chromatography (stationary phase: silica gel, eluent: CH_2Cl_2).

2.2 Analytical methods and instrumentation

NMR spectra were acquired at 298 K with a Varian Mercury Plus VX 400 (^{1}H, 399.9; ^{13}C, 100.6 MHz), or a Varian Inova 600 (^{1}H, 599.7; ^{13}C, 150.8 MHz) spectrometers. Chemical shifts were internally referenced to residual solvent peaks. Full ^{1}H- and ^{13}C-NMR assignments were accomplished, if necessary, with the aid of gHSQC and gHMBC NMR experiments using standard Varian pulse sequences. Infrared spectra were acquired at 298 K on a Perkin-Elmer Spectrum 2000 FT-IR spectrophotometer. Elemental analyses were performed on a Thermo-Quest Flash 1112 Series EA instrument ESI-MS spectra were obtained by dissolving samples in MeOH or CH_3CN and injecting the resulting solution into a Waters Micromass ZQ 4000.

*2.3 Synthesis of pre-catalysts **3b-d***

*2.3.1 Synthesis of cyclopentadienone ruthenium complexes ion paired to imidazolium salts **3b,c**.*

The dimeric precursor dicarbonyl (η^4-3,4-bis-(4-methoxyphenyl)-2,5-diphenylcyclopenta-2,4-dienone) (**2**) was individually reacted with the imidazolium salts **1b**,**c** (2 equiv. vs. **2**). A quantitative fast reaction led to the formation of the ionic pair composed of the imidazolium cations and the metal anionic complexes derived from the coordination of the imidazolium halide counterion to the ruthenium center. Reaction mixtures were partially dried under vacuum and precipitation with hexane followed by filtration yielded the products as yellow powders.

[dicarbonyl(η^4-3,4-bis(4-methoxyphenyl)-2,5-diphenylcyclopenta-2,4-dienone)(iodine)ruthenium] [1,2,3-trimethyl-imidazolium] (3b): 1,2,3-trimethyl-imidazolium iodide (**1b**) 0.079 g (0.332 mmol) and **2** 0.200 g (0.166 mmol) were mixed in inert atmosphere and left stirring in CH_2Cl_2 at room temperature for1h. The product (**3b**) was obtained as a yellow solid with a yield of 93%. Complex **3b** is stable to air, moisture, in solution of organic solvents and in the presence of water. **3b** was analyzed by IR, ^{1}H-NMR, ^{13}C-NMR and ESI-MS. ^{1}H-NMR (400MHz, $CDCl_3$): δ 7.55 (d, CH_{aryl}, 4H), 7.15 (s, 2H, CH_{im}), 7.11-6.96 (m, CH_{aryl}, 10H), 6.55 (d, CH_{aryl}, 4H), 3.70 (s, OCH_3, 3H), 3.58 (s, -NCH_3, 6H), 2.45 (s, -NCH_3N-, 3H). ^{13}C-NMR (150.8 MHz, $CDCl_3$): δ

201.74 (CO), 172.05 (C=O, Cp), 158.29 (-$COCH_3$), 143.97 (-$NC(CH_3)N$-), 135.50-112.60 (C_{aryl}), 127.13 (CH_{Im}), 100.47 ($C_{2,5}$, Cp), 80.88 ($C_{3,4}$, Cp), 54.99 (-OCH_3), 35.87 (NCH_3), 10.91 (-$NC(CH_3)N$-). IR (CH_2Cl_2 cm^{-1}): 2000, 1940 (νCO), 1592 (νC=O), 1607, 1517 (νC=C). ESI-MS (m/z) (+): 111 $[ImMe_3]^+$; (-): 729 {$[Ru(CO)_2ICpO]^-$}. Anal. Calcd (%) for $C_{39}H_{35}IN_2O_5Ru$: C, 55.79; H, 4.20; N, 3.34. Found: C, 55.72; H, 4.16; N, 3.39.

[dicarbonyl(η^4-3,4-bis(4-methoxyphenyl)-2,5-diphenylcyclopenta-2,4-dienone)(chloro)ruthenium][1,3-bis(2,6-diisopropylphenyl)imidazolium] (3c): 1,3-bis(2,6-diisopropylphenyl)imidazolium chloride (**1c**) 0.141 g (0.332 mmol), and **2** 0.200 g (0.166 mmol) were mixed in inert atmosphere and left stirring in CH_2Cl_2 at room temperature for 1h. The product (**3c**) was obtained as a yellow solid with a yield of 89%. Complex **3c** is stable to air, moisture, in solution of organic solvents and in the presence of water. **3c** was analyzed by IR, ^{1}H-NMR, ^{13}C-NMR, ESI-MS. ^{1}H-NMR (599.7 MHz, $CDCl_3$): δ 8.15 (s, NCHN), 7.97 (s, 2H, CH_{Im}), 7.65-6.53 (CH_{aryl}), 3.69 (s, 6H, -OCH_3), 2.43 (sept., J = 6.8 Hz, 4H, CH_{iPr}), 1.28 (d, J = 6.8 Hz, 12H, CH_{3iPr}), 1.12 (d, J = 6.8 Hz, 12H, CH_{3iPr}). ^{13}C-NMR (150.8 MHz, $CDCl_3$): δ 201.74 (CO), 170.88 (C=O, Cp), 158.13 (-$COCH_3$), 135.25 (NCHN), 145.14-112.48 (C_{aryl}), 128.28 (CH_{im}), 99.94 ($C_{2,5}$, Cp), 80.54 ($C_{3,4}$, Cp), 54.93 (-OCH_3), 28.84 (CH_{iPr}), 24.72 (CH_3iPr), 23.77 (CH_{3iPr}). IR (CH_2Cl_2, cm^{-1}): 2000, 1937 (νCO); 1591 (νC=O), 1607, 1517 (νC=C). ESI-MS (m/z) (+): 389 $[ImIPr]^+$; (-) 637 {$[Ru(CO)_2ClCpO]^-$}, 609 {$[Ru(CO)_2ClCpO]^-$-CO}. Anal. Calcd (%) for $C_{60}H_{61}ClN_2O_5Ru$: C, 70.19; H, 5.99; N, 2.75. Found: C, 70.21; H, 6.01; N, 2.77.

2.3.2 Synthesis of a cyclopentadienone ruthenium complex ion paired to tetraethylammonium.

[dicarbonyl(η4-3,4-bis(4-methoxyphenyl)-2,5-diphenylcyclopenta-2,4-dienone)(iodine)ruthenium] [tetraethylammonium] (3d): tetraethyl ammonium iodide 0.085 g (0.332 mmol), and **2** 0.200 g (0.166 mmol were mixed under inert atmosphere and left stirring in CH_2Cl_2 at room temperature. After 2 h the solvent was removed under vacuum and the crude was washed twice with H_2O (20mL). Then, the solid was dissolved in the minimum amount of CH_2Cl_2

and precipitated with hexane. The product (**3d**) was obtained as a yellow solid with a yield of 90%. Complex **3d** is stable to air, moisture, in solution of organic solvents and in the presence of water. **3d** was analyzed by IR, ^{1}H-NMR, ^{13}C-NMR, ESI-MS. ^{1}H-NMR (400MHz, $CDCl_3$): δ 7.52 (d, CH_{aryl}, 4H), 7.17-7.06 (m, CH^{aryl}, 10H), 6.61 (d, CH_{aryl}, 4H), 3.68 (s, OCH_3, 6H), 3.15 (quart, -NCH_2-, 8H), 1.20 (tripl, -CH_3, 12H). ^{13}C-NMR (150.8 MHz, $CDCl_3$): δ 201.28 (CO), 171.97(C=O, Cp), 158.27 (-$COCH_3$), 135.40-112.60 (C_{aryl}), 100.15 ($C_{2,5}$, Cp), 80.67 ($C_{3,4}$, Cp), 55.02 (-OCH_3), 52.62 (-NCH_2), 7.77 (-CH_3). IR (CH_2Cl_2, cm^{-1}): 1999, 1939 (νCO), 1591 (νC=O), 1607, 1517 (νC=C). ESI-MS (m/z) (+): 130 $[TEA]^+$; (-): 729 $\{[Ru(CO)_2ICpO]^-\}$. Anal. Calcd (%) for $C_{41}H_{44}INO_5Ru$: C, 57.34; H, 5.16; N, 1.63. Found: C, 57.41; H, 5.22; N, 1.61.

*2.4 Synthesis of the dinuclear complex **4(Na)***

[(η^5-$Ph_4C_4COHOCC_4Ph_4$-η^5)(μ-H)[$(CO)_4Ru_2$] Shvo's complex **4(H)** (0.083 g, 0.0689 mmol) was mixed with sodium ethoxide (0.0490 g, 5 equiv. per ruthenium atom) in ethanol under inert atmosphere. After stirring for 1 h at reflux temperature, the solvent was removed under vacuum. The residue was then dissolved in dichloromethane and precipitated with hexane obtaining a light green powder **4(Na)** with a yield of 82%. The solid was analysed by FT-IR, ^{1}H-NMR, ^{13}C-NMR, ESI-MS. ^{1}H-NMR (400MHz, $CDCl_3$): δ 7,11-6,54 (CH_{aryl}), 3.70 (s, 12H, -OCH_3), -16,08 (s, 1H, Ru-H). ^{13}C-NMR (150.8 MHz, $CDCl_3$): δ 201.91 (CO), 159.76 (C=O, Cp), 158.88 (-$COCH_3$), 133.13-112.85 (C_{aryl}), 101.82 ($C_{2,5}$, Cp), 85.61 ($C_{3,4}$, Cp), 55.03 (-OCH_3). IR (CH_2Cl_2, cm^{-1}): 2021, 1991, 1951 (νCO); 1588 (νC=O), 1607, 1517 (νC=C). ESI-MS (m/z) (+) 1229 $[M+H]^+$, 1251 $[M+Na]^+$, 1267 $[M+K]^+$.

*2.5 Synthesis of the ruthenium hydride complex **3c-H***

[dicarbonyl(η4-3,4-bis(4-methoxyphenyl)-2,5-diphenylcyclopenta-2,4-dienone)(hydride)ruthenium][1,3-bis(2,6-diisopropylphenyl)imidazolium] (3c-H): Imidazolium salt **1c** (0.0570 g, 0.135 mmol) was mixed with with potassium tert-butoxide (0.0228 g, 0.203 mmol) in anhydrous THF under inert atmosphere. The solution was stirred for 1 h at room

temperature, then the solvent was removed under vacuum and the residue re-dissolved in toluene. After filtration, the organic solution was vacuum dried yielding the corresponding carbene (0.0520 g 0.133 mmol). The carbene was dissolved in 5 ml of ^{i}PrOH and **2** (0.0407 g, 0.0338 mmol) was added to the solution at reflux temperature. After 30 minutes of reaction, the solvent was removed under vacuum and the residue dissolved in EtOAc and precipitated with hexane. The orange solid was obtained in quantitative yield by filtration and identified as **3c-H** by FT-IR, ^{1}H-NMR, ^{13}C-NMR, ESI-MS. ^{1}H-NMR (400MHz, acetone-d_6): δ 8.28 (s, NCHN), 7,68 (s, 2H, CH_{Im}), 7.65-6.54 (CH_{aryl}), 3.66 (s, 6H, -OCH_3), 2.59 (sept., J = 6.3 Hz, 4H, CH_{iPr}), 1.28 (d, J = 6.8 Hz, 12H, CH_{3iPr}), 1.14 (d, J = 6.8 Hz, 12H, CH_{3iPr}), -9,94 (s, 1H, Ru-H). ^{13}C-NMR (150.8 MHz, toluene d_8): δ 207.44 (CO), 171.33 (C=O, Cp), 158.32 (-$COCH_3$), 134.96 (NCHN), 145.49-112.73 (C_{aryl}), 126.88 (CH_{im}), 102.86 ($C_{2,5}$, Cp), 84.10 ($C_{3,4}$, Cp), 54.15 (-OCH_3), 28.94 (CH_{iPr}), 24.11 (CH_{3iPr}). IR (CH_2Cl_2, cm^{-1}): 1976, 1909 (νCO); 1600 (νC=O), 1607, 1518 (νC=C). ESI-MS (m/z) (+): 389 $[ImIPr]^+$; (-) 603 $\{[Ru(CO)_2HCpO]^-\}$.

2.6 General procedure for upgrading of EtOH with co-catalyst

Each catalytic run was carried out in an oven-dried 6mL Schlenk bomb fitted with a Teflon plug valve. The reactor was loaded with the ruthenium catalyst **3a** (0.0172 mmol), the base (NaOEt or NaOMe or NaOH), 1.72 mmol) and the co-catalyst (BQ-OMe or BQ). Finally, ethanol (0.500 mL, 8.60 mmol) was added under inert atmosphere. The Schlenk bomb was sealed under inert atmosphere and heated at 150 °C, unless otherwise specified, under magnetic stirring for the suitable reaction time. After cooling with an ice-water bath, the microreactor was opened and the reaction mixture was diluted by 4.5 mL of Et_2O. THF (150 uL) was added as internal standard. Ethanol conversion and product yields were determined by injecting the resulting solution (0.5 uL) into an Agilent Technologies 7890A GC system using a HP-5 capillary column Agilent 190915-413 (30 m x 0.35 mm, thickness 0.25 μm). Helium was used as carrier gas with a column flow of 0.909mL/min; the injector was kept at a temperature of 230 °C in split mode (40:1); total flow was

40.25 mL/min. The method used was: starting oven temperature 30°C (hold for 11 min), ramp to 270 at 30°C/min (held for 5 min). All products were calibrated. THF (150 μL) was added to different solutions of alcohols at increasing concentration and the ratio A_a/A_s vs mol_a was plotted (mol_s = constant) . This way the measure of the total reaction volume can be avoided.

Compounds were also identified by GC-MS, using an Agilent Technologies 6890 GC coupled with a mass spectrometer Agilent Technologies 5973 equipped with a non-polar column (5% Phenyl - 95% methylsiloxane), 30m x 250 μm x 1.05 μm. The volume of solution injected was 0.5 μL. Helium was used as carrier gas with a column flow rate of 1mL/min; the injector was maintained at a temperature of 250 °C in split mode (50:1); total flow was 23.9 mL/min. The temperature program was the following: isothermal step at 40 °C for 7 minutes, then ramp to 250 °C at 10 °C/min, final isothermal step for 5 minutes. Light compounds were studied by sampling the headspace of the reactor at room temperature. A portion of gas phase (0.5 mL) was injected into the aforementioned GC-MS system and analyzed using the following temperature program: isothermal step at 40 °C (held for 10 minutes), then ramp to 220 °C at 10 °C/min, final isothermal step for 2 minutes. Hydrogen was detected by means of an Agilent Technologies 7890A GC equipped with a thermal conductivity detector (TCD) and a HP-molesieve column (30m x 0,53 mm x 50 μm). Nitrogen was used as carrier gas at a flow rate of 3 mL/min; the injector was maintained in split mode 5:1 at a temperature of 150 °C and the TCD at 150 °C. The volume of gas injected was 0.04 mL and the standard temperature program was a single isothermal step at 50 °C for 5 minutes. The injection of pure reference standards allowed the comparison of retention times in the GC and GC-MS columns.

2.6.1 Recycle experiment

An oven-dried 6 mL Schlenk bomb fitted with a Teflon plug valve was loaded with the ruthenium catalyst **3a** (0.0172 mmol), NaOEt (1.72 mmol) and BQ (0.129 mmol). Ethanol (0.500 mL, 8.60 mmol) was added under inert atmosphere and the reactor was sealed. The resulting reaction mixture was heated, under stirring, at 150 °C for 4h. After cooling at room temperature, the alcohol mixture

was removed under vacuum. Finally, new aliquots of EtOH (0.500 mL, 8.60mmol), NaOEt (1.72 mmol) and BQ (0.129 mmol) where appropriate were added under inert atmosphere to the solid residue and the following cycle was carried out as previously outlined.

3. Results and discussion

3.1 Screening of ruthenium-based ionic pre-catalysts.

A small library of pre-catalysts was prepared by exploiting the reactivity of variously functionalized imidazolium salts (**1b,c**) with the dinuclear complex (η^4-3,4-bis-(4-methoxyphenyl)-2,5-diphenylcyclopenta-2,4-dienone) (**2**) previously reported by the group (Scheme 1),[29, 31] with the principal aim to assess a possible role of the imidazolium cation in the catalytic reaction for **3a-3c** (*vide infra*). Furthermore, **2** was reacted with tetraethylammonium (TEA) iodide leading to the quantitative formation of **3d**.

The synthesis of **3b–d** can be easily monitored by IR spectroscopy, observing in all the cases a lowering in the CO stretching frequencies (e.g. **3b**: ν(CO) = 2000, 1940 cm^{-1} vs. **2**: 2018, 1967 cm^{-1}) with respect to **2**. IR spectra of ion pairs **3c** and **3d** are very similar to that of complex **3b**. The lower stretching frequency suggests the negative charge is more localized on the metal center rather than on the cyclopentadienone ligand carbonyl group. DFT analysis based on natural atomic charges[32] supports this picture, showing a larger increase of negative charge on Ru than on the cyclopentadienone oxygen when comparing **3a** (considering both the isolated anion species and the tight ion pair) with the neutral dimer **2** (see Table S1).

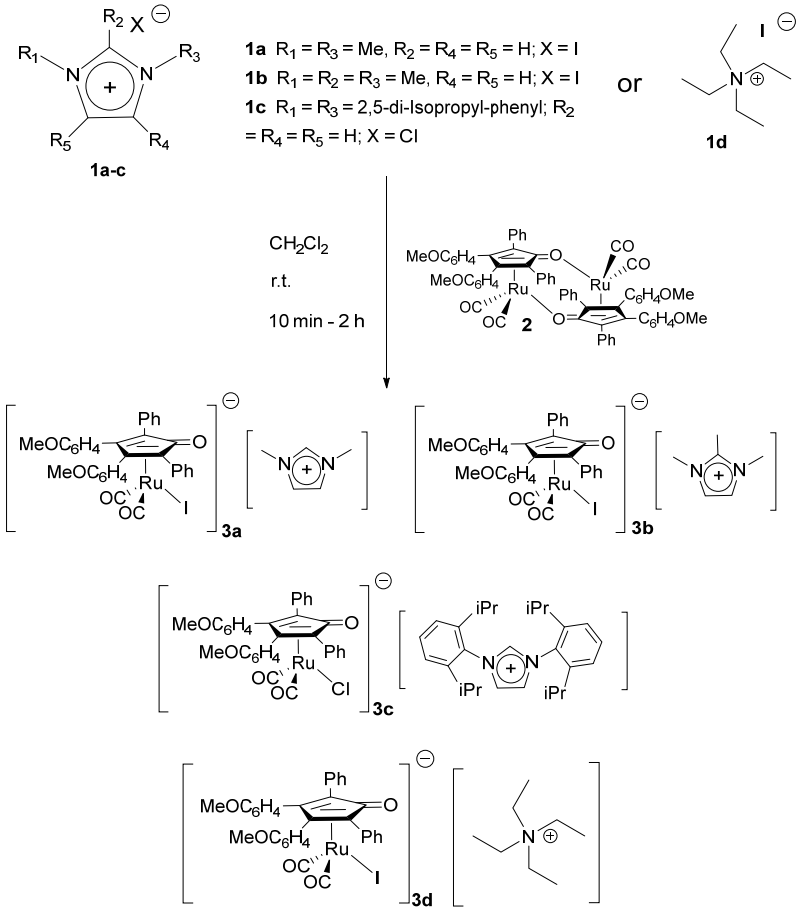

Scheme 1. Pre-catalysts **3a**[29] and **3b-d** employed in this work.

The η^4coordination of the cyclopentadienone ring is thus reasonable, and the negative charge on the metal ion together with the σ-donor nature of the halogen ion allow more back-bonding toward the CO ligands. This observation is confirmed by the C=O distance in the X-ray diffraction of single crystals obtained for the complex **3a** (1.242(7) Å).

Despite the **3a** negative charge not being largely accumulated on the cyclopentadienone, the solid state structure of **3a** (Figure 1) comprising $[\{2,5\text{-}Ph_2\text{-}3,4\text{-}(p\text{-}MeO\text{-}C_6H_4)_2(\eta^4\text{-}C_4C{=}O)\}Ru(CO)_2I]^-$ complex anions and imidazolium $[1,3\text{-}Me_2\text{-}C_3N_2H_3]^+$ cations, shows an inter-molecular C41-H1···O3 (C41-H41 0.93 Å, H41···O3 2.16 Å, C41···O3 2.958(10) Å, <C41H41O3 143.1°) hydrogen bond. The molecular structures of the cation and anion closely resemble those previously reported for related salts.[31] The presence of the same inter-molecular C41-H1···O3 interaction also in ethanol solution is supported by DFT computations, with even stronger hydrogen bond

(C41-H41 1.09 Å, H41···O3 1.86 Å, C41···O3 2.85 Å and <C41H41O3 147.3°) and with the imidazolium and the coordinated iodide lying closer than in the crystal (see Figure. S1). The η^4 coordination of the cyclopentadienone ligand is corroborated by the fact that the Ru1-C3 distance [2.499(7) Å] is sensibly longer than in Ru1-C4 [2.245(7) Å], Ru1-C5 [2.201(7) Å], Ru1-C6 [2.202(6) Å] and Ru1-C7 [2.250(6) Å], with similar differences obtained by DFT computations (ca. 0.26 Å, in average), confirming the same (η^4) coordination in ethanol solution.

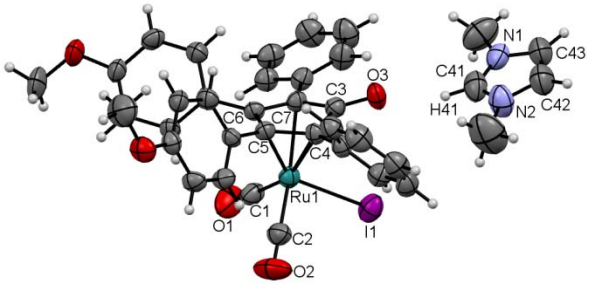

Figure. 1. ORTEP drawing of **3a**. Displacement ellipsoids are at the 30% probability level. Selected bond lengths (Å) and angles (°): Ru1-C1 1.900(8), Ru1-C2 1.880(8), Ru1-C3 2.499(7), Ru1-C4 2.245(7), Ru1-C5 2.201(7), Ru1-C6 2.202(6), Ru1-C7 2.250(6),C1-O1 1.115(7), C2-O2 1.151(8), C3-O3 1.242(7), N1-C41 1.307(9), N2-C41 1.312(9), N1-C43 1.358(9), N2-C42 1.337(9), C42-C43 1.343(11), Ru1-C1-O1 175.7(7), Ru1-C2-O2 179.0(8), C4-C3-C7 104.7(6), C3-C4-C5 107.9(6), C4-C5-C6 107.9(6), C5-C6-C7 108.7(6), C6-C7-C3 107.8(6), C41-N1-C43 107.0(8), C41-N2-C42 106.7(8), N1-C41-N2 111.1(8), N1-C43-C42 106.7(8), N2-C42-C43 108.6(9). H-bond C41-H41···O3: C41-H41 0.93 Å, H41···O3 2.16 Å, C41···O3 2.958(10) Å, <C41H41O3 143.1°.

^{1}H-NMR and ^{13}C-NMR spectra show the typical pattern of the starting reagents moved to different chemical shifts. A more significant indication of the structure reported in Scheme 1 is given by ESI-MS analyses, which show the molecular anion $[Ru(CO)_2\{C_5(C_6H_4OMe)_2(Ph)_2{=}O\}(X)]^-$ and the corresponding molecular cation. (See experimental).

Pre-catalysts **3b-d** have been tested in the Guerbet reaction (Table 1) under the best performing conditions previously optimized for **3a** (entry 1).[29] Pre-catalyst **3b,** bearing a methyl group on the -NCN- carbon of the imidazolium ring, leads to a ca. 19% decrease in ethanol conversion (27%, **3b**, entry 2 vs 46%, **3a**, entry 1) with a concomitant decline in alcohols' selectivity (**3b**, 70%, vs **3a**, 91%). Regarding **3c**, it is noticeable how the presence of bulky substituents on the heteroatoms affects the catalytic activity. In particular, a high drop in conversion is observed (entry 3: from 46% for **3a** to 17% for **3c**). Analogously, by replacing the imidazolium salt with a non-protic counterion such as tetraethylammonium (TEA) **3d** (entry 4), an impressive drop in alcohols yield together with a substantial increase in the carbon loss are observed. This overall evidence preliminarily suggest a role of the imidazolium salt.

Table 1. Guerbet reaction catalyzed by type **3** complexes. Conditions: cat (0.2 mol%); NaOEt (20 mol%) T = 150 °C; P autogenous; t = 4 h.

Entry	Cat	Conv. EtOH (%)	Yield BuOH (C_4) (%)	Alcohols yield (C_4-C_{10}) (%)[a]	C-loss (%)
1[29]	**3a**	46	32	42	3
2	**3b**	27	15	19	8
3	**3c**	17	9	11	6
4	**3d**	37	10	11	25

[a]Alcohols yield corresponds to the sum of C_4-C_{10} saturated alcohols.

It is important to underline that the role of basic media in the Guerbet reaction is likely to prevent the formation of the mononuclear active species $[Ru(CO)_2\{C_5(C_6H_4OMe)_2(Ph)_2\text{-}OH\}(H)]$ responsible for the H-transfer mechanism in several reactions where Shvo type pre-catalysts are employed.[34-40] Indeed, by refluxing the Shvo complex **4(H)** with EtONa in EtOH for 1h (Scheme 2), the dimeric complex **4(Na)** is quantitatively formed, in which the acidic hydrogen is replaced by a sodium cation.

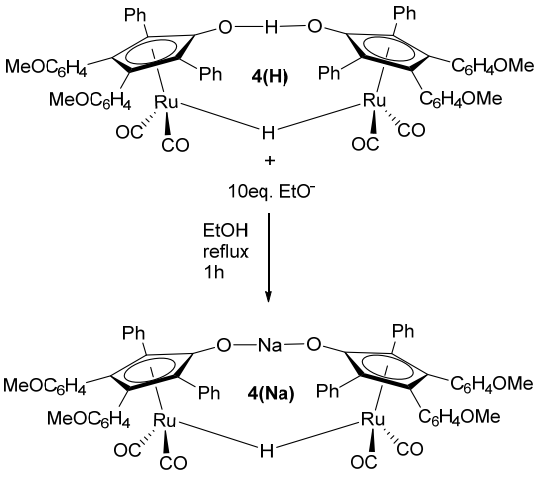

Scheme 2. Quantitative formation of the dimeric complex **4(Na)** from the reactivity of Shvo complex and NaOEt.

In fact, the IR spectrum of **4(Na)** shows three bands in the CO region which are shifted to lower frequencies compared to **4(H)** (**4(Na)**: ν(CO) = 2021, 1991, 1951 cm^{-1} vs. **4(H)**: 2036, 2005, 1977 cm^{-1}) suggesting a similar molecular symmetry. Notably, DFT geometry optimization confirmed the structural stability of **4(Na)** and the corresponding simulated IR spectra reproduced the red shifts of CO vibrations with respect to **4(H)** (see Table S2 in the SI). Furthermore, ^{1}H-NMR spectroscopy confirmed the presence of a bridging hydride at δ -16,1 ppm and ESI-MS shows the molecular ion at m/z = 1229 [M+H^{+}] (see experimental and SI for further characterization).

As recently reported by our group, Shvo pre-catalyst **4(H)**, which is likely to convert on the pre-catalyst **4(Na)** under Guerbet conditions, works by far worse (Shvo – conv EtOH: 17%; C loss: 10%) than **3a** (entry 1, table 1) [29] further suggesting a possible role of the imidazolium salt in the catalytic cycle.

Great research effort has been devoted to the rationalization of the pKa of imidazolium salts vs substituents, both from an experimental[41] and a theoretical point of view.[42,43] In general, most values are available in DMSO or water solution and define that imidazolium salts with aromatic substituents have lower pKa than alkyl substituted ones. Furthermore, it is generally recognized that counterions do not affect the acidity of the -NCHN- proton. Thus, we can expect that the

imidazolium salt in precursor **3c** will be more acidic than in precursor **3a**. On the other hand, pKa values of imidazolium salts (pKa ~ 20-23) are generally higher than that of EtOH (pKa ~ 16). On these premises, it is reasonable to affirm that in EtOH solution NaOEt would form a buffer system with the solvent rather than deprotonating the heterocyclic compound.

By excluding the classic Shvo complex as a precursor and considering a possible role of the imidazolium salt, which is likely to remain protonated, a simplified catalytic cycle can be drawn as in scheme 3 (path **A**).

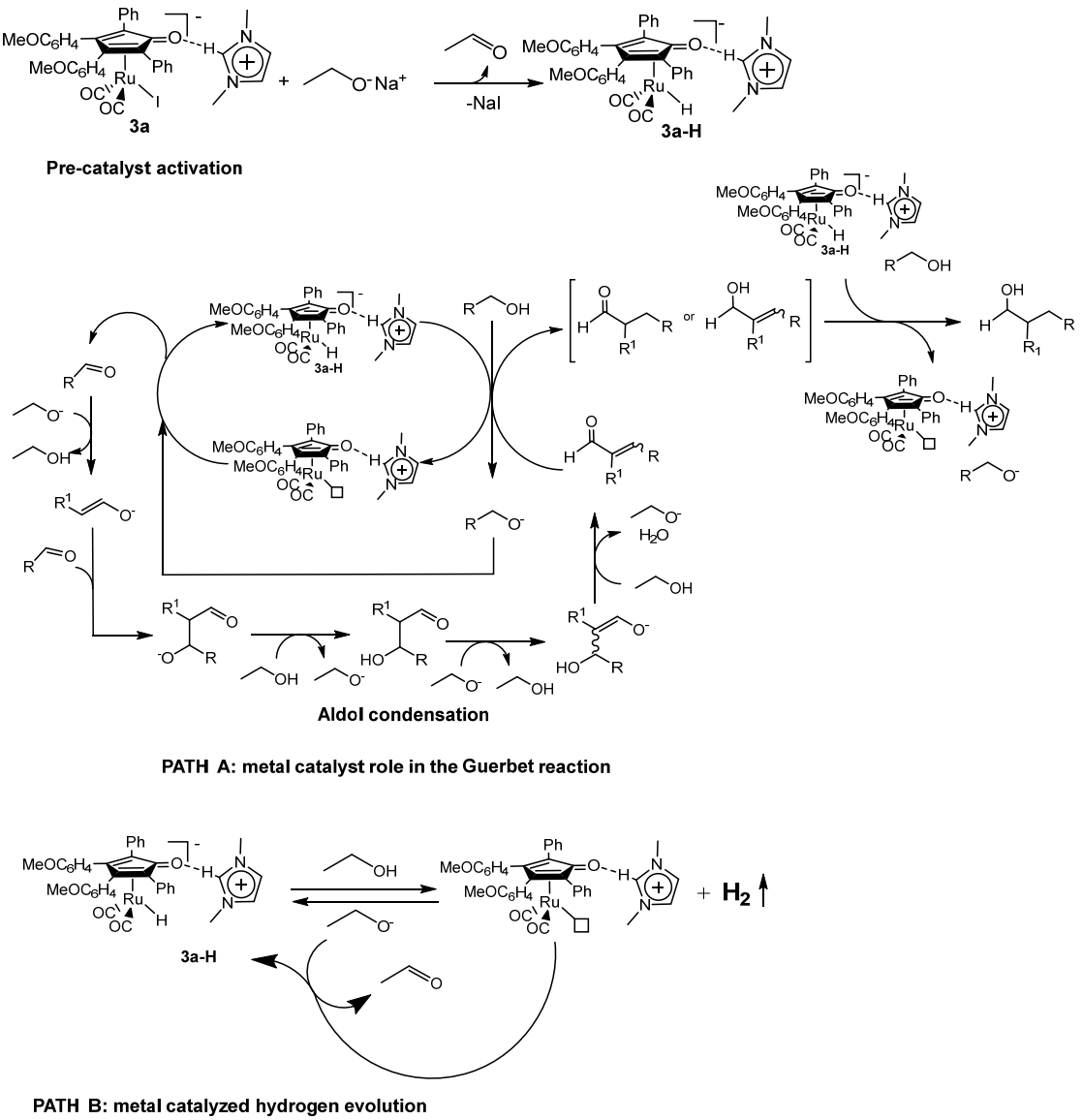

Scheme 3. Proposed pathway for the Guerbet reaction (path **A**) catalyzed by **3a** (R = alkyl chain, C1-C9) and the concurrent hydrogen evolution (path **B**).

Imidazolium salts are particularly prone to form hydrogen bonding with polar solvents, especially when containing an acidic proton on the -NCN- carbon as in **3a** and **3c**.[44-46] Although we could speculate about several interactions between the cation, the anion or the ionic couple in the reaction mixture, a complete interpretation of the effect of any possible interaction on the catalytic system' behavior is not trivial due to the intrinsic complexity. Still, DFT computations provided information on the structural stability of the tight ion pairs of **3a** and **3c** in solution, along with their corresponding hydride species, **3a-H** and **3c-H** (Figure 2). In fact, as described above for **3a**, the anionic species interact closely with the imidazolium proton in a H-bond fashion, and this happens also if the cation comprises encumbered aromatic N-substituents, as in **3c**. Notably, this interaction also exists (and it is even stronger) in the optimized geometries of the hydride species **3a-H** and **3c-H**, suggesting that formation of tight ion-pairs is promoted not only by electrostatics but also by specific H-bond interactions, overcoming steric hindrances of imidazolium cations.

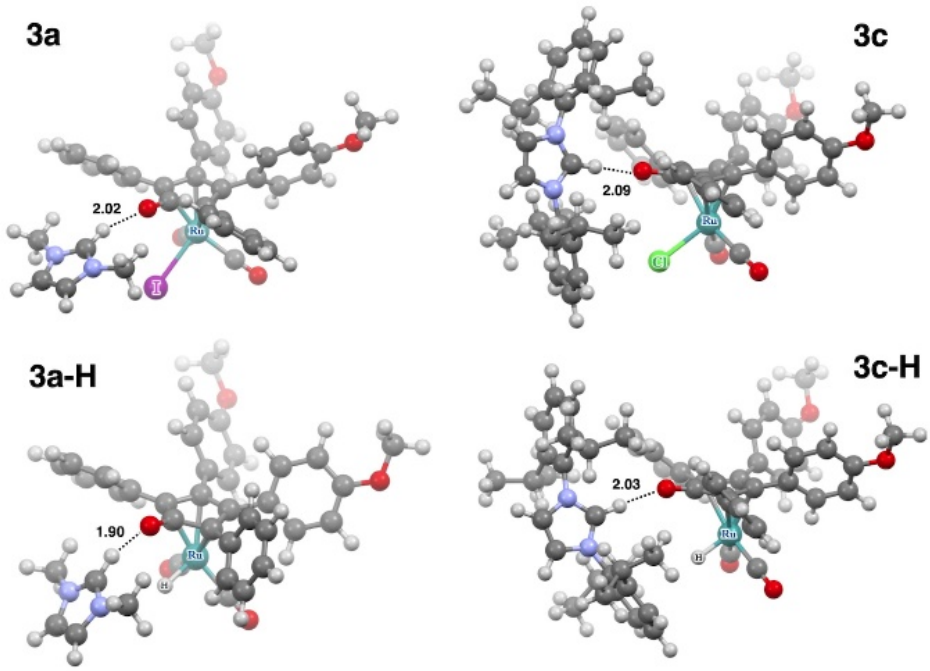

Figure 2. DFT optimized structures for the **3a**, **3c**, **3a-H** and **3c-H** complexes in ethanol.

Although a hydride species was detected via ^{1}H-NMR (δ = -9.86 ppm) and IR spectroscopy revealed the presence of a new set of IR bands in the CO region (υ(CO)= 1984, 1916 cm^{-1}) when employing **3a** as catalyst, the resting state was difficult to completely characterize experimentally due to the complexity and instability of the reaction mixture. To further confirm the structure of the hypothesized intermediate **3a-H,** a stable hydride ionic couple **3c-H** was isolated by reacting the corresponding carbene in EtOH with the ruthenium dimer **2** (Scheme 4).

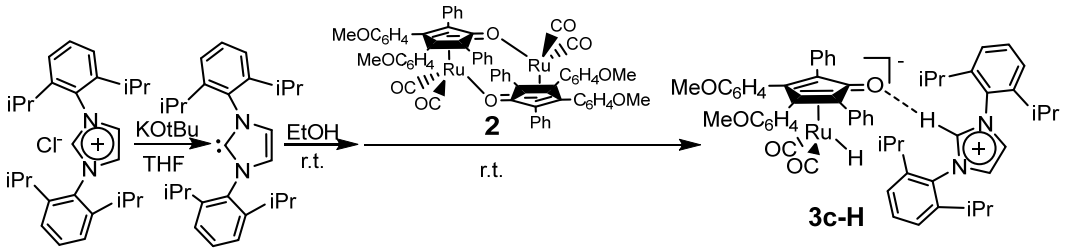

Scheme 4. Isolated Ru-hydride species **3c-H**.

^{1}H-NMR experiments revealed both the –NC*H*N- proton (δ 8.78 ppm corresponding to the -N*C*HN- signal at δ 135 ppm in ^{13}C-NMR) [29, 31] of the imidazolium salt and the terminal Ru-hydride (δ ($CDCl_3$) = -9,94 ppm) at typical chemical shifts (see also experimental and SI). Once again, the two CO stretches were found at lower frequencies in comparison to **3c** (**3c-H**: υ(CO) = 1976, 1909 cm^{-1} vs **3c**: υ(CO) = 2000, 1937 cm^{-1}). DFT simulated IR spectra confirmed these red-shifts associated with hydrides formation as shown in Table S3 in the SI. Such evidence agrees with the higher σ-donor ability of the hydride ion compared to the chloride ligand. ESI-MS confirmed the presence of both the anionic molecular ion at 603 m/z and the molecular cation at 389 m/z.

In addition, by performing the Guerbet reaction with complex **3c-H** (cat 0.2 mol%, 150 °C, NaOEt = 20 mol%, 4 h), the detrimental effect of the encumbered N-substituted imidazolium salt is confirmed [conv EtOH = 16%, yield BuOH = 8%, alcohol yield = 12%, carbon loss = 5%].

Having all the above described information in our hands, we can preliminarily draft a role of hydrogen bond on the hydrogenation/dehydrogenation activity of **3a-H** and **3c-H**. From an electronic point of view, the stronger the hydrogen bond (**3aH** 1.90 Å vs **3cH** 2.03 Å, Figure 2), the

higher the CO stretching (**3a-H** = 1984, 1916 cm^{-1} and **3c-H** = 1976, 1909 cm^{-1}) which decreases increasing backbonding. In line with this notion **3a-H** shows an higher hydride donor ability (see Table S1), which should accelerate reduction [34] and conversely decelerate the dehydrogenation step. This behaviour may affect the production rate of acetaldehyde, likely favouring the equilibria between dehydrogenation, aldol condensation and hydrogenation in the Guerbet reaction (assuming that the faster is the dehydrogenation, the higher should be the acetaldehyde which converts to C-loss before condensation).

Noteworthy, GC analyses provided evidence for a significant content of molecular hydrogen in the final headspace of the reaction vessel (Figure 3). This suggests an important contribution of the parallel hydrogen evolution reaction (Scheme 1, path **B**). Except for **3c,** which is poorly active in both hydrogenation and dehydrogenation reactions, hydrogen evolution is likely similar for all the other counter-cations. As previously reported,[29] acetaldehyde is also identified in the gas phase in traces.

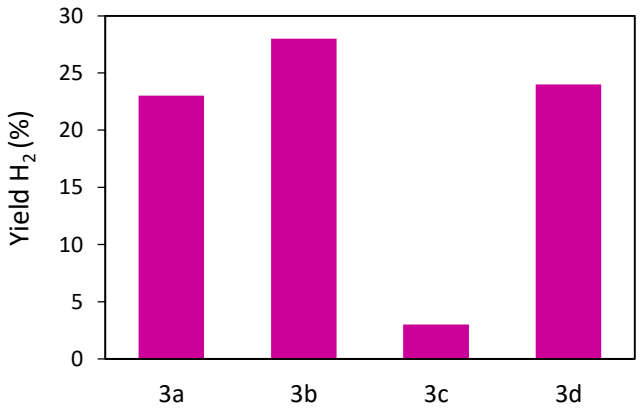

Figure 3. Hydrogen evolution registered in the Guerbet reaction catalyzed by **3a-3d** (cat 0.2 mol%, NaOEt 20 mol% of base, T = 150°C, t= 4h)

Concerning the H_2 evolution, it is important to underline that if it derived from the dehydrogenation of the only ethanol, the H_2 percentage should be lower than C-loss in Table 1. This incongruence can be explained taking into consideration hydrogen that could come from the co-catalyst NaOEt in

the presence of water from condensation. This can be accounted separately by the ethanol carbon balance, in a parasite reaction that consumes the base co-catalyst, namely NaOEt + H_2O that leads to NaOAc + $2H_2$. This appears to be also promoted by **3a-3d** (dehydrogenation catalysts) as reported by Beller and co-workers for ruthenium pincer catalysts exploited for H_2 production from EtOH in water under basic (OH^-) conditions.[47]

3.2 Boosting the Guerbet reaction with benzoquinone as co-catalyst

Taking inspiration from the biomimetic aerobic alcohol oxidations developed by Backvall and co-workers with a coupled Shvo/Co-salen catalytic system[48, 49] and with the principal aim to gain better control on the hydrogen evolution step, we decided to augment our catalytic system by adding an electron transfer mediator, such as 2,6-dimethoxy-1,4-benzoquinone (BQ-OMe), as a co-catalyst (1.5 mol%).

To our delight, no H_2 release was observed at the end of the reaction. Furthermore, a significant boost in the overall reaction efficiency was registered (Table 2).

For **3a** (entry 1 in Table 1 vs entry 2 in Table 2) a gain of 19% in alcohols yield is observed. Selectivity in butanol shows a slight decline (70% for **3a**, vs 52% for **3a**/BQ-OMe), but the decrease in total higher alcohols selectivity is less pronounced (91% for **3a** vs 85% for **3a**/BQ-OMe), suggesting that the co-catalyst favors the production of higher alcohols rather than butanol, as expected at higher conversion. Although a carbon loss of 7-13% is affecting the final mixtures, the efficiency of the catalytic system is overall enlarged and dehydrogenation toward H_2 production (path **B** in Scheme 3) is completely avoided. Increasing the reaction time (Table 2, entry 3) did not lead to any improvement.

Table 2. Guerbet reaction with 2,6-dimethoxybenzoquinone (BQ-OMe, 1.5%) as co-catalyst. Conditions: **3a** (0.2 mol%); NaOEt (20 mol%); T = 150 °C; P autogenous.

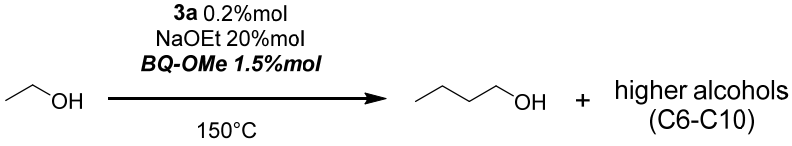

entry	t	Conv. EtOH (%)	Yield BuOH (C_4) (%)	Alcohols yield (C_4-C_{10}) (%)[a]	C-loss (%)
1	20 min	58	32	51	7
2	4 h	72	38	61	11
3	24 h	73	34	60	13

[a] Alcohols yield corresponds to the sum of C_4-C_{10} saturated alcohols.

3.2.1 Screening of the reaction conditions

Screening of the reaction temperatures confirmed the behavior observed in the absence of a co-catalyst.[29] Lowering the temperature (entry 1 in Table 3) to 80 °C led to a turn-off of the Guerbet process, with almost all converted ethanol contributing to the carbon loss. At an intermediate temperature of 110 °C (entry 2), the overall conversion is still low and the carbon loss is around half of the conversion. In the same way, an increase in the operative temperature (180 °C, entry 4) revealed a detrimental effect, thus prompting us to choose 150 °C (entry 3) as the temperature for the new catalytic system as well.

Table 3. Guerbet reaction with 2,6-dimethoxybenzoquinone (BQ-OMe, 1.5%) as co-catalyst. Conditions: **3a** (0.2 mol%); NaOEt (20 mol%). P autogenous.

Entry	T (°C)	Conv. EtOH (%)	Yield BuOH (C_4) (%)	Alcohols yield (C_4-C_{10}) (%)[a]	C-loss (%)
1	80	19	1	1	18
2	110	23	10	13	10
3	150	72	38	61	11
4	180	54	25	39	25

[a] Alcohols yield corresponds to the sum of C_4-C_{10} saturated alcohols.

Other pre catalysts such as **3b** showed a very limited improvement of the conversion and alcohol yield (Table 4, entry 1 vs Table 1, entry 2) along with a furtherly increased carbon loss. On the other hand, the behavior of the Shvo catalyst **4(H)** seems to be completely unaffected by the co-catalyst (Table 4, entry 2)

Table 4. Guerbet reaction with 2,6-dimethoxybenzoquinone (BQ-OMe, 1.5%) as co-catalyst. Conditions: cat (0.2 mol%); NaOEt (20 mol%) T = 150 °C, P autogenous.

Entry	Cat	Conv. EtOH (%)	Yield BuOH (C_4) (%)	Alcohols yield (C_4-C_{10}) (%)[a]	C-loss (%)
1	**3b**	41	14	23	18
2	**4(H)**	15	3	5	10

[a] Alcohols yield corresponds to the sum of C_4-C_{10} saturated alcohols.

Analyzing the data in Figure 4, the upgrade in conversion and alcohol yields upon BQ-OMe addition (ruthenium catalyst **3a**) can be transferred to other bases such as NaOMe and NaOH (conversion: +26% with NaOEt, +18% with NaOMe, +36% with NaOH) (C_4-C_{10} yields: +19% with NaOEt, +12% with NaOMe, +27% with NaOH).

NaOMe, as expected, entered the reaction favoring the production of odd alcohols, and in general this species negatively affects the carbon balance favoring the production of heavy species. [29] Nevertheless NaOH improves the conversion, leading to a concurrent increase of the carbon loss.

In order to further comment on this latter data, it has to be firstly stated that the primary side process that affects the homogeneous Guerbet process is the Cannizzaro reaction, which turns off the reaction by converting the co-catalytic base NaOEt in sodium acetate. This is also the case for **3a**/BQ-OMe system. Indeed, by collecting, weighting and analyzing by ^{1}H-NMR the water soluble fraction of the solid at the end of the catalytic run (reaction condit ions: **3a**: 0.2 mol%; NaOEt: 20 mol%; BQ-OMe: 1.5 mol%; T: 150 °C; t: 4h, Table 2, entry 2), the only presence of sodium acetate and sodium butanoate in a 1:10 ratio was detected (see figure S22 in the SI). Being the weight of the solid 0.144 g (corresponding to 1.70 mmol in acetates) and the amount of NaOEt employed 1.72

mmol, it is reasonable to state that the base is quantitatively converted into acetates. This is consistent with the Cannizzaro reaction that affects the Guerbet process, leading to the base co-catalyst consumption. Thus, this part of the solid, which represents the quantitative transformation of the base co-catalyst, can be considered apart from the ethanol carbon balance, namely from the C-loss reported in Tables, which refers independently to the starting material ethanol (8.3 mmol). This assumption has been followed in all the literature available for homogeneous Guerbet catalytic reactions where this aspect is discussed.[24-29] Finally, the carbon loss attributable to ethanol conversion could be ascribable to oligomerization of aldehydes to heavy insoluble products and to unsaturated intermediates hardly detectable from the GC and GC-MS analyses.

On the other hand, NaOH under the conditions in Figure 4 converts the 20% of the feedstock (8.3 mmol of EtOH) into NaOEt and water in order to have the substrate available for the Cannizzaro reaction. This behavior is finally affecting the conversion and carbon loss from ethanol which increase by 20%. However, taking into account that NaOH has some advantages respect to NaOEt, the overall efficiency of this base in the presence of BQ-OMe is anyway remarkable.

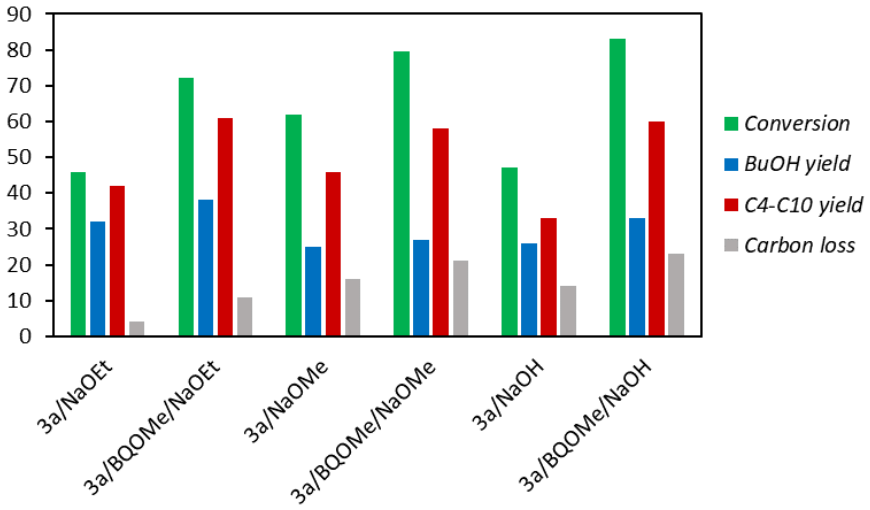

Figure 4. Base screening for the Guerbet reaction promoted by catalyst **3a**[27] and new system **3a**/BQ-OMe Reaction conditions: T = 150 °C, autogenous pressure, t = 4 h, base = 20 mol%.

Quite surprisingly, GC-MS analyses of the final reaction mixture revealed the presence of odd alcohols even when bases different from NaOMe were employed (Figure S23). Actually, BQ-OMe

under the reaction condition can be expected to lose -OMe moieties,[50] which later enter themselves in the catalytic cycle.

To avoid this co-catalyst reactivity and to check the influence of electron-withdrawal on the co-catalyst, 1,4-benzoquinone (BQ) and 2,3-dichloro-1,4-naphthoquinone (NQ) were subsequently tested. As expected, no trace of odd-alcohol was detected. While electron-withdrawing groups negatively affect the conversion, (Table 5, entry 2), nice performances were registered when using unsubstituted benzoquinone (Table 5, entry 1).

Table 5. Guerbet reaction with different co-catalysts. Conditions: **3a** (0.2 mol%); NaOEt (20 mol%); T = 150 °C; t = 4 h; P autogenous.

Entry	Additive	Conv. EtOH (%)	Yield BuOH (C_4) (%)	Alcohols yield (C_4-C_{10}) (%)[a]	C-loss (%)
1	BQ	79	39	63	16
2	NQ	41	24	32	10

[a] Alcohols yield corresponds to the sum of C_4-C_{10} saturated alcohols.

Table 6 displays screenings of **3a**/BQ system at different reaction times. By comparing Table 2 with Table 6, although at a first sight BQ (Table 6, entry 2, C-loss 16%) has a detrimental effect on the reaction selectivity with respect to BQ-OMe (Table 2, entry 2, C-loss 11%), increasing the reaction time reduces the carbon loss (Table 6, entry 3, selectivity in C4-C10 = 96%). This is likely to be attributed to the presence of unreacted intermediates after 4 h with 1.5% of BQ, requiring a longer reaction time to be completely converted into valuable alcohols. This latter behavior is not registered for BQ-OMe (Table 2) which decreased in performance over time, actually making BQ an even better candidate for our purposes.

Table 6. Guerbet reaction with benzoquinone (BQ, 1.5%) as co-catalyst. Conditions: **3a** (0.2 mol%); NaOEt (20 mol%); T = 150 °C; P autogenous.

Entry	t	Conv. EtOH (%)	Yield BuOH (C_4) (%)	Alcohols yield (C_4-C_{10}) (%)[a]	C-loss (%)
1	20 min	51	31	48	3
2	4 h	79	39	63	16
3	24 h	78	38	75	3

[a] Alcohols yield corresponds to the sum of C_4-C_{10} saturated alcohols.

Noteworthy, the latter data makes **3a**/BQ system the best result ever reported for the Guerbet reaction. [26, 51]

Screenings on the loading of BQ unveil that increasing the amount (Table 7, entry 3 and 4) does not improve the overall efficiency. On the contrary although leading to a lower conversion (68%), decreasing the BQ loading to 0.5% (Table 7, entry 1) leads to a negligible carbon loss after 4 h. (Table 7, entry 2).

Table 7. Guerbet reaction with benzoquinone (BQ) as co-catalyst. Conditions: **3a** (0.2 mol%); NaOEt (20 mol%); T = 150 °C; t = 4 h. P autogenous.

entry	BQ (mol%)	Conv. EtOH (%)	Yield BuOH (C_4) (%)	Alcohols yield (C_4-C_{10}) (%)[a]	C-loss (%)
1	0.5	68	38	67	1
2	1.5	79	39	63	16
3	5	72	39	62	11
4	12	55	31	47	6

[a] Alcohols yield corresponds to the sum of C_4-C_{10} saturated alcohols.

Halving the loading of the catalyst **3a** to 0.1 mol% does not affect the catalytic activity (Table 8). However, a lower efficiency is obtained with 0.02 mol% of **3a**. The best TON of 670 is reached with **3a** (0.1 mol%) / BQ (0.5 mol%) (entry 1).

Table 8. Guerbet reaction with benzoquinone (BQ) as co-catalyst. Conditions: **3a** (0.2 mol%); NaOEt (20 mol%); T = 150 °C; t = 4 h. P autogenous.

entry	3a (%)	BQ (%)	Conv. EtOH (%)	Yield BuOH (C_4) (%)	Alcohols yield (C_4-C_{10}) (%)[a]	C-loss (%)
1	0.1	0.5	69	36	67	2
2	0.1	1.5	76	34	66	10
3	0.02	0.5	38	21	32	6
4	0.02	1.5	48	26	41	7

Even more outstanding results were finally obtained by changing the base loading. Since doubling the base percentage without the use of an additive represented a detriment in selectivity (conv. 75%, carbon loss 21%),[29] **3a**/BQ system was tested with 40% of NaOEt (Figure 5). This time, the overall conversion shows a further 5% increase and selectivity is almost completely directed toward butanol and higher alcohols already after 4 h (Figure 5, b). Increasing the reaction time up to 8 h (Figure 5, c) improves the conversion to 88%, with an overall selectivity in higher alcohols (C4-C10) of 97% (Figure 5, c), the highest obtained up to date.

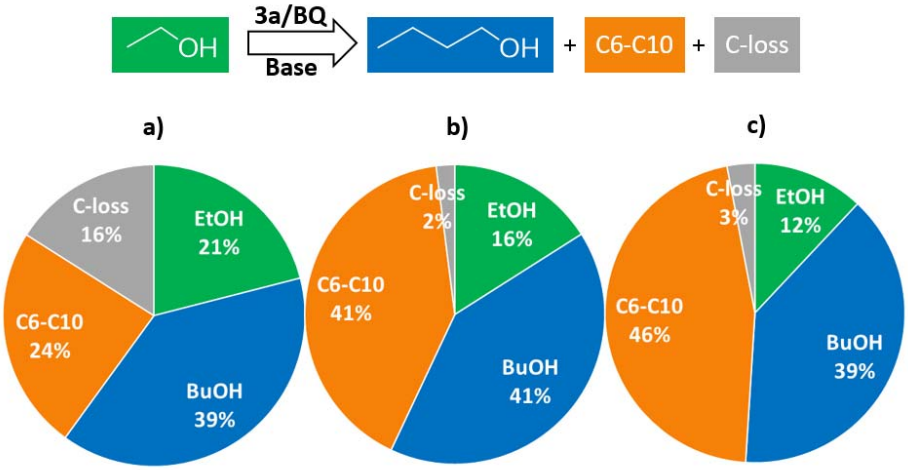

Figure 5. Effect of NaOEt quantity on the reaction: composition of the final reaction mixtures. Catalytic system: **3a**/BQ (0.2 mol%/1.5 mol%). Co-catalyst: NaOEt, a) 20 mol%; t = 4 h b) 40 mol%; t = 4 h c) 40 mol%; t = 8 h. T = 150 °C, autogenous pressure.

*3.2.2. Reactivity of **3a**/BQ system toward real matrixes*

The negative effect of water on selectivity with **3a** alone [29] is also prevented in the presence of the additive BQ. By diluting EtOH with 30% of H_2O under the conditions of Table 7 (entry 2) led to a conversion of 59% associated to yield in C_4-C_{10} alcohols of 58% (yield 1-BuOH = 38%).

Eventually, the behavior of the optimized catalytic system **3a**/BQ was studied towards real matrixes, more specifically two waste mixtures containing EtOH and by-products (Table 9). The first one, being absolute alcohol (entry 2), showed yield in alcohols comparable to pure EtOH supplied by Merck, while the use of EtOH CAVIRO 95% (entry 3), a waste sample deriving from heads and tails of ethanol distillation, provided a satisfactory behavior, in line with the experiment above described with EtOH/H_2O. Noteworthy, the presence of several by-products in the CAVIRO 95% sample (see Table 9 and S4 for mixture composition) makes it useless for any other purposes but incineration. Noticeably, not only do such by-products not largely affect the catalytic system activity toward the bio-refinery process, but indeed, as in the case of aldehydes, they take part in mixture valorization being themselves intermediates in the Guerbet reaction.

Table 9: Effect of the EtOH starting material on the reaction. Catalyst system: complex **3a**/BQ (0.2 mol%/1.5 mol%). Co-catalyst: NaOEt, 20 mol% respect to EtOH. T = 150 °C, autogenous pressure.

entry	EtOH[a]	Conv. EtOH (%)	Yield BuOH (C_4) (%)	Alcohols yield (C_4-C_{10}) (%)[b]	C-loss (%)
1	Merck	79	39	63	16
2	Caviro AA	80	38	72	8
3	Caviro 95%[c]	66	37	63	3

[a] EtOH pure: Merck purchaser (code: 24105-1L-M), EtOH CAVIRO: see batch analyses (Table S4); [b] Alcohols yield corresponds to the sum of C_4-C_{10} saturated alcohols. [c] The 5% is composed by several alcohols, aldehydes, esters and ketones.

3.2.3 Proposed catalytic cycle

Summarizing the information obtained from the screening of **3a**/BQ system, a synergic role of **3a** and BQ in the process can be depicted. A possible role of BQ as a catalytic "hydrogen storage" agent is also likely. Furthermore, the acidity of hydroquinone is higher than that of EtOH, thus we can expect at least a partial deprotonation toward its basic form. From this information, we can draw a plausible simplified catalytic cycle as reported in Scheme 5.

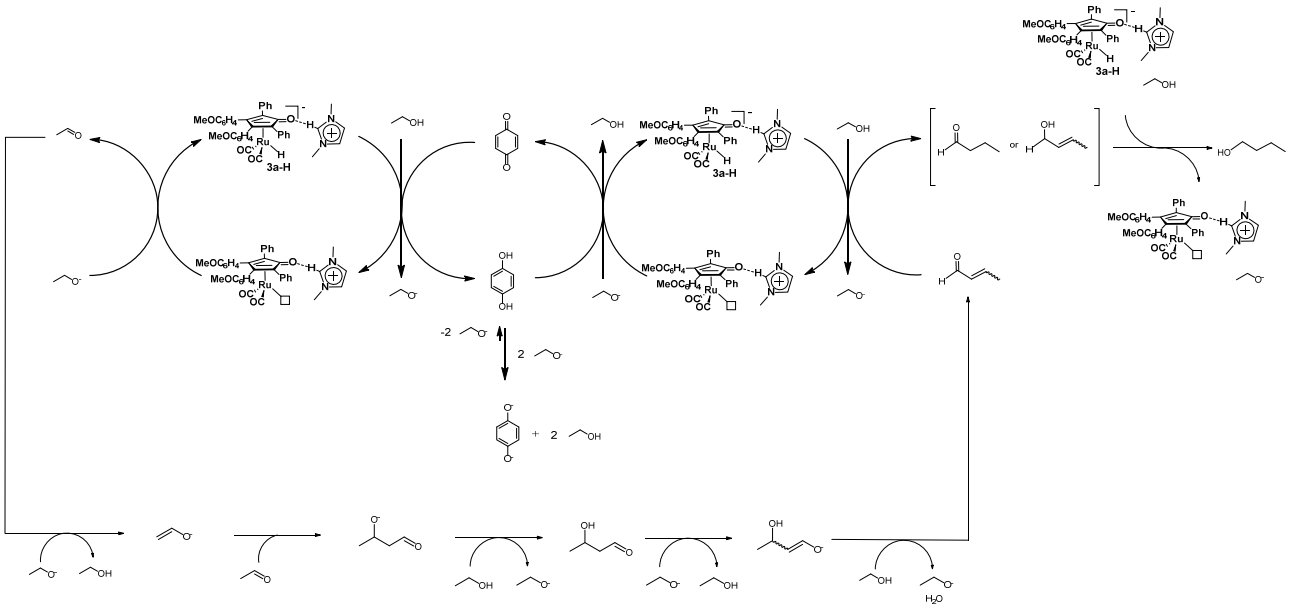

Scheme 5. Proposed pathway for the Guerbet reaction catalyzed by the system **3a**/BQ and the concurrent hydrogen evolution.

Benzoquinone is likely to enter the catalytic cycle in the oxidation of **3a-H** assisted by a molecule of EtOH. Later on, hydroquinone (in equilibrium with its deprotonated counterpart) would be prone to undergo re-oxidation by the 16 electrons intermediate represented with a vacant site and by the base (EtO^-). At this point, **3a-H** is restored and available for the hydrogenation of aldehydes after aldol condensation, thus closing the catalytic cycle.

*3.2.4 Catalytic system **3a**/BQ recycling*

Two recycle experiments were performed: the first one (light blue bar in Figure 6) was carried out by removing the alcohol mixture under vacuum at the end of the first cycle, re-loading a new portion of EtOH and NaOEt to the reaction vessel and then reacting again at 150 °C for 4 hours.

This way, the catalytic system **3a**/BQ can be recycled with good efficiency. Contrarily, the re-addition of fresh BQ to the dry mixture negatively affects the recycle (orange bar in Figure 6). This latter behavior agrees with results obtained from the screening of the BQ loading (Table 7). The conversion of the catalytic system is indeed negatively affected by the increase of the BQ percentage, further confirming that BQ (1.5% mol) is not deactivated under the reaction conditions employed.

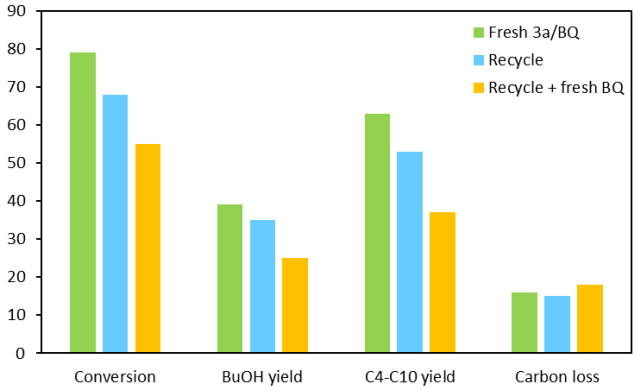

Figure 6. Catalytic system recycle. Catalytic system: complex **3a**/BQ (0.2 mol%/1.5 mol%).Reaction conditions: T = 150 °C, autogenous pressure, t = 4 h, base = 20 mol%.

The catalytic system **3a**/BQ does not deactivate with the reaction: working with a TON of 315 (under conditions of Figure 6) within the first cycle, it maintains a TON of 265 when reused. This behavior further confirms the base responsibility in the reaction switch off by means of the Cannizzaro reaction as reported for complex **3a**.[29]

4. Conclusions

Reactivity, supported by DFT calculations, of ionic ruthenium catalysts **3a-3d** and dimeric complexes **4(H)** and **4(Na)** highlights a participation of the imidazolium counterion, 1,3-dimethylimidazolium giving the best performance, in the Guerbet reaction efficiency. Furthermore DFT computations provide information on the formation of tight ion-pairs for **3a** and **3c** promoted not only by electrostatics but also by specific H-bond interactions in solution. Interactions that become even stronger for their corresponding hydride species **3a-H** and **3c-H.**

The screening of different counterions also sheds light on the parallel hydrogen evolution which subtracts substrate from the Guerbet reaction mechanism.

The reaction scheme includes the dehydrogenation of ethanol into acetaldehyde (the only reaction occurring on ethanol with our catalytic system, neither ethylene nor diethylether were detected), and the transformation of the aldehyde into either 1-butanol or higher saturated alcohols, with consumption of the hydrogen generated in the first step. The C-loss and the positive hydrogen yield, found especially in the absence of the benzoquinone co-catalyst, were mainly due to side reactions occurring on acetaldehyde, such as the Cannizzaro and oligomerization.

The addition of a catalytic amount of a benzoquinone derivative (1,4-benzoquinone being the most efficient) to the reaction mixture (catalytic system **3a**/BQ) gives an impressive boost to the reaction, solving several drawbacks. The first and most important one is to delete hydrogen evolution, which is completely avoided. The hydrogen cost thus becomes null as in an ideal Guerbet reaction. In fact, all the hydrogen coming from ethanol dehydrogenation is restored in the last step, hydrogenation of aldehydes, likely passing through the benzoquinone/hydroquinone as a "storage" system during aldol condensation.

The reaction occurs without additional solvent (another good deal for atom economy) in the presence of an inorganic base as a condensation co-catalyst leading to unprecedented conversions and yields with very high selectivity: maximum conversion of 88% associated to alcohols yield of 85% and an overall selectivity in higher alcohols of 97%.

The reaction is barely affected by the presence of water and **3a**/BQ system shows a greater water tolerance if compared with **3a**.

From an industrial application perspective, the cooperative **3a**/BQ catalytic process can be transferred to a real matrix. In fact, when employing heads and tails from ethanol distillation (supplier: CAVIRO distillery) no significant change in the composition of the final reaction mixture

is observed. Employing bio-ethanol from waste in the process would represent a closing step in the circular economy of wine and distillates production chain.

Apart from few drawbacks in the recycling phase which are currently under investigation, **3a**/BQ catalytic system paves the way for the development of a sustainable process answering to the current topic of second-generation biofuel production.

Acknowledgements

We gratefully acknowledge "Valsovit project" with the contribution of the Emilia Romagna Region through POR FERS 2014-2020 funds (European Regional Development Fund) and the University of Bologna. The company CAVIRO s.r.l (namely Dr. Rosa Prati and Ing. Giovanni Marani) deserve a special acknowledgement for furnishing the waste ethanol real mixtures. IR gratefully acknowledges the use of HPC resources of the "Pôle Scientifique de Modélisation Numérique" (PSMN) of the ENS-Lyon, France.

Supporting Information.

Characterization data for all products, including ^{1}H, ^{13}C NMR and ESI-MS spectra. GC chromatogram for selected experiments. Composition of the ethanol waste real matrix. Crystallography data for CCDC 2087771. DFT calculation details. This material is available free of charge via the Internet at http://pubs.acs.org.

Abbreviations

LCA life cycle assessment, TEA tetraethylammonium, NaOEt sodium ethoxide, NaOAc sodium acetate, EtOH ethanol, BuOH butanol, Cn alcohol containing n carbon atoms, conv. Conversion, C-loss carbon loss, BQ-OMe 2,6-dimethoxy-1,4-benzoquinone, BQ 1,4-benzoquinone. NQ 2,3-dichloro-1,4-naphthoquinone.

References

[1] C. Angelici, B. M. Weckhuysen, P. C. A. Bruijnincx, Chemocatalytic Conversion of Ethanol into Butadiene and Other Bulk Chemicals, ChemSusChem 6 (2013) 1595–1614.

[2] J. A. Posada, A. D. Patel, A. Roes, K. Blok, A. P. C. Faaij, M. K. Patel, Potential of Bioethanol as a Chemical Building Block for Biorefineries: Preliminary Sustainability Assessment of 12 Bioethanol-Based Products, Bioresour. Technol. 135 (2013) 490–499.

[3] P. C. A. Bruijnincx, B. M. Weckhuysen, Shale Gas Revolution: An Opportunity for the Production of Biobased Chemicals?, Angew. Chem. Int. Ed. 52 (2013) 11980–11987.

[4] J. Pang, M. Zheng, L. He, L. Li, X. Pan, A. Wanga, X. Wang, T. Zhang, Upgrading ethanol to n-butanol over highly dispersed Ni–MgAlO catalysts, J. Catal. 344 (2016) 184–193.

[5] S. Hanspal, Z. D. Young, J. T. Prillaman, R. J. Davis, Influence of surface acid and base sites on the Guerbet coupling of ethanol to butanol over metal phosphate catalysts, J. Catal. 352 (2017) 182–190.

[6] T. W. Birky, J. T. Kozlowski, R. J. Davis, Isotopic transient analysis of the ethanol coupling reaction over magnesia, J. Catal. 298 (2013) 130–137

[7] M. K. Akhtar, H. Dandapani, K. Thiel, P. R. Jones, Microbial Production of 1-Octanol: A Naturally Excreted Biofuel with Diesel-like Properties, Metab. Eng. Commun. 2 (2015) 1–5.

[8] J. Campos-Fernández, J. M. Arnal, J. Gómez, M. P. A. Dorado, Comparison of Performance of Higher Alcohols/diesel Fuel Blends in a Diesel Engine, Appl. Energy 95 (2012) 267–275.

[9] G. M. Torres, R. Frauenlob, R. Franke, A. Borner, Production of Alcohols via Hydroformylation, Catal. Sci. Technol. 5 (2015) 34–54.

[10] J. T. Kozlowski, R. J. Davis, Heterogeneous Catalysts for the Guerbet Coupling of Alcohols, ACS Catal. 3 (2013) 1588–1600.

[11] D. Gabriëls, W. Y. Hernández, B. Sels, P. Van Der Voort, A. Verberckmoes, Review of Catalytic Systems and Thermodynamics for the Guerbet Condensation Reaction and Challenges for Biomass Valorization, Catal. Sci. Technol. 5 (2015) 3876–3902.

[12] Q. Zhang, J. Dong, Y. Liu, Y. Wang, Y. Cao, Towards a Green Bulk-Scale Biobutanol from Bioethanol Upgrading, J. Energy Chem. 25 (2016) 907–910.

[13] A. Chieregato, J. V. Ochoa, C. Bandinelli, G. Fornasari, F. Cavani, M. Mella, On the Chemistry of Ethanol on Basic Oxides: Revising Mechanisms and Intermediates in the Lebedev and Guerbet Reactions, ChemSusChem 8 (2015) 377–388.

[14] C. R. Ho, S. Shylesh, A. T. Bell, Mechanism and Kinetics of Ethanol Coupling to Butanol over Hydroxyapatite, ACS Catal. 6 (2016) 939–948.

[15] T. L. Jordison, L. Peereboom, D. J. Miller, Impact of Wa-ter on Condensed Phase Ethanol Guerbet Reactions, Ind. Eng. Chem. Res. 55 (2016) 6579–6585.

[16] Z. Sun, A. C. Vasconcelos, G. Bottari, M. C. A. Stuart, G. Bonura, C. Cannilla, F. Frusteri, K. Barta, Efficient Catalytic Conversion of Ethanol to 1-Butanol via the Guerbet Reaction over Copper- and Nickel-Doped Po-rous Solids, ACS Sustain. Chem. Eng. 5 (2017) 1738–1746.

[17] G. R. M. Dowson, M. F. Haddow, J. Lee, R. L. Wingad, D. F. Wass, Catalytic Conversion of Ethanol into an Advanced Biofuel: Unprecedented Selectivity for n-Butanol, Angew. Chem. Int. Ed. 52 (2013) 9005 –9008.

[18] H. Aitchison, R. L. Wingad, D. F. Wass, Homogeneous Ethanol to Butanol Catalysis - Guerbet Renewed, ACS Catal. 6 (2016) 7125–7132.

[19] S. Fu, Z. Shao, Y. Wang, Q. Liu, Manganese-Catalyzed Upgrading of Ethanol into 1-Butanol, J. Am. Chem. Soc. 139 (2017) 11941–11948.

[20] N. V. Kulkarni, W. W. Brennessel, W. D. Jones, Catalytic Upgrading of Ethanol to N-Butanol via Manganese-Mediated Guerbet Reaction, ACS Catal. 8 (2018) 997–1002.

[21] Y. Liu, Z. Shao, Y. Wang, L. Xu, Z. Yu, Q. Liu, Manganese Catalyzed Selective Upgrading of Ethanol with Methanol into Isobutanol, ChemSusChem 12 (2019) 3069 – 3072.

[22] K. S. Rawat, S. C. Mandal, P. Bhauriyal, P. Garg, B. Pathak, Catalytic upgrading of ethanol to n-butanol using an aliphatic Mn–PNP complex: theoretical insights into reaction mechanisms and product selectivity, Catal. Sci. Technol., 9 (2019) 2794–2805.

[23] A. M. King, H. A. Sparkes, R. L. Wingad, D. F. Wass, Manganese Diphosphine and Phosphinoamine Complex-es Are Effective Catalysts for the Production of Biofuel Alcohols via the Guerbet Reaction, Organometallics 39 (2020) 3873−3878.

[24] K.-N. T. Tseng, S. Lin, J. W. Kampf, N. K. Szymczak, Upgrading Ethanol to 1-Butanol with a Homogeneous Air-Stable Ruthenium Catalyst, Chem. Commun.52 (2016) 2901–2904.

[25] S. Chakraborty, P. E. Piszel, C. E. Hayes, R. T. Baker, W. D. Jones, Highly Selective Formation of N-Butanol from Ethanol through the Guerbet Process: A Tandem Catalytic Approach, J. Am. Chem. Soc. 137 (2015) 14264–14267.

[26] Y. Xie, Y. Ben-David, L. J. W. Shimon, D. Milstein, Highly Efficient Process for Production of Biofuel from Ethanol Catalyzed by Ruthenium Pincer Complexes, J. Am. Chem. Soc. 138 (2016) 9077–9080.

[27] A. Ohligschlager, N. van Staalduinen, C. Cormann, J. Muhlhans, J. Wurm, M. A. Liauw, The Guerbet Reaction Network – a Ball-in-a-Maze-Game or: Why Ru-MACHO-BH is Poor in Coupling two Ethanol to n-Butanol, Chemistry—Methods 1 (2021) 181 –191.

[28] K. J. Pellow, R. L. Wingad, D. F. Wass, Towards the Up-grading of Fermentation Broths to Advanced Biofuels: A Water Tolerant Catalyst for the Conversion of Ethanol to Isobutanol, Catal. Sci. Technol. 7 (2017) 5128–5134.

[29] R. Mazzoni, C. Cesari, V. Zanotti, C. Lucarelli, T. Tabanelli, F. Puzzo, F. Passarini, E. Neri, G. Marani, R. Prati, F. Vigano, A. Conversano, F. Cavani, Catalytic Biorefining of Ethanol from Wine

Waste to Butanol and Higher Alcohols: Modeling the Life Cycle Assessment and Pro-cess Design, ACS Sustain. Chem. Eng. 7 (2019) 224−237.

[30] C. Cesari, S. Conti, S. Zacchini, V. Zanotti, M. C. Cassani, R. Mazzoni, Sterically driven synthesis of ruthenium and ruthenium–silver N-heterocyclic carbene complexes, Dalton Trans. 43 (2014) 17240–17243.

[31] C. Cesari, A. Cingolani, M. Teti, A. Messori, S. Zacchini, V. Zanotti, R. Mazzoni, Imidazolium Salts of Ruthenium Anionic Cyclopentadienone Complexes: Ion Pair for Bi-functional Catalysis in Ionic Liquids, Eur. J. Inorg. Chem. (2020) 1114–1122.

[32] A. E. Reed, R. B. Weinstock, F. Weinhold, Natural-population analysis, J. Chem. Phys. 83 (1985) 735-746.

[33] Warner, J-E. Backvall, Mechanistic Aspects on Cyclopentadienylruthenium Complexes in Catalytic Racemization of Alcohols, Acc. Chem. Res. 46 (2013) 2545–2555.

[34] B. L. Conley, M. K. Pennington-Boggio, E. Boz, T. J. Williams, Discovery, Applications, and Catalytic Mechanisms of Shvo ’s Catalyst, Chem. Rev. 110 (2010) 2294−2312.

[35] C. Cesari, L. Sambri, S. Zacchini, V. Zanotti, R. Mazzoni, Microwave-Assisted Synthesis of Functionalized Shvo-Type Complexes, Organometallics 33 (2014) 2814−2819.

[36] T. Pasini, G. Solinas, V. Zanotti, S. Albonetti, F. Cavani, A. Vaccari, A. Mazzanti, S. Ranieri, R. Mazzoni, Substrate and Product Role in the Shvo’s Catalyzed Selective Hydrogenation of the Platform Bio-Based Chemical 5-Hydroxymethylfurfural, Dalton. Trans. 43 (2014) 10224−10234.

[37] C. Cesari, A. Cingolani, C. Parise, S. Zacchini, V. Zanotti, M. C. Cassani, R. Mazzoni, Ruthenium Hydroxycyclopentadienyl N-Heterocyclic Carbene Complexes as Transfer Hydrogenation Catalysts, RSC Adv. 5 (2015) 94707−94718.

[38] C. Cesari, R. Mazzoni, H. Müller-Bunz, M. Albrecht, Ruthenium (0) complexes with triazolylidene spectator ligands: Oxidative activation for (de)hydrogenation catalysis, J. Organomet. Chem. 793 (2015) 256–262.

[39] C. Cesari, R. Mazzoni, E. Matteucci, A. Baschieri, L. Sambri, M. Mella, A. Tagliabue, F. L. Basile, C. Lucarelli, Hydrogen Transfer Activation via Stabilization of Coordinatively Vacant Sites: Tuning Long-Range π-System Electronic Interaction between Ru(0) and NHC Pendants, Organometallics 38 (2019) 1041–1051.

[40] C. Cesari, R. Conti, A. Cingolani, V. Zanotti, M. C. Cassani, L. Rigamonti, R. Mazzoni, Synthesis and Reactivity of Poly(propyleneimine) Dendrimers Functionalized with Cyclopentadienone N-Heterocyclic-Carbene Ruthenium(0) Complexes, Catalysts 10 (2020) 264.

[41] M. H. Dunn, N. Konstandaras, M. L. Cole, J. B. Harper, Targeted and systematic approach to the study of pKa values of imidazolium salts in dimethylsulfoxide, J. Org. Chem. 82 (2017) 7324-7331.

[42] Z. Wang, Y. Zheng, Y. Zheng, X.-S. Xue, P. Ji, A systematic theoretical study on the acidities for cations of ionic liquids in dimethyl sulfoxide, J. Phys. Chem. A. 122 (2018) 5750-5755.

[43] E. Rossini, A. D. Bochevarov, E. W. Knapp, Empirical conversion of pKa values between different solvents and interpretation of the parameters: application to water, acetonitrile, dimethylsulfoxide, and methanol, ACS Omega 3 (2018) 1653-1662.

[44] H. K. Stassen, R. Ludwig, A. Wulf, J. Dupont, Imidazolium Salt Ion Pairs in Solution, Chem. Eur. J. 21 (2015) 8324 – 8335.

[45] X. Zhu, H. Sun, D. Zhang, C. Liu, Theoretical study on the interactions between methanol and imidazolium-based ionic liquids, J. Mol. Model. 17 (2011) 1997–2004.

[46] P. A. Hunt, C. R. Ashworth, R. P. Matthews, Hydrogen bonding in ionic liquids, Chem. Soc. Rev. 44 (2015) 1257—1288.

[47] P. Sponholz, D. Mellmann, C. Cordes, P. G. Alsabeh, B. Li, Y. Li, M. Nielsen, H. Junge, P. Dixneuf, and M. Beller, Efficient and Selective Hydrogen Generation from Bioethanol using Ruthenium Pincer-type Complexes, ChemSusChem 7 (2014) 2419 – 2422.

[48] E. V. Johnston, E. A. Karlsson, L.-H. Tran, B. Akermark, J.-E. Backvall, Efficient Aerobic Ruthenium-Catalyzed Oxidation of Secondary Alcohols by the Use of a Hybrid Electron Transfer Catalyst, Eur. J. Org. Chem. (2010) 1971–1976.

[49] S. Albonetti, R. Mazzoni, F. Cavani, Homogeneous, heterogeneous and nanocatalysis in Transition metal catalysis in aerobic alcohol oxidation, Ed. Francesca Cardona and Camilla Parmeggiani (2015) RSC Green Chemistry, Royal Society of Chemistry.

[50] R. Gulaboski, I. Bogeski, V. Mirceski, S. Saul, B. Pasieka, H. H. Haeri, M. Stefova, J. P. Stanoeva, S. Mitrev, M. Hoth, R. Kappl, Hydroxylated derivatives of di-methoxy-1,4-benzoquinone as redox switchable earth-alkaline metal ligands and radical scavengers, Scientific Reports 3 (2013) 1865.

[51] F. Cavani, V. Zanotti, R. Mazzoni, C. Lucarelli, C. Cesari, T. Tabanelli, F. Puzzo, Improved process for the transformation of primary aliphatic alcohols into higher aliphatic alcohols, patent WO2019193079 (A1) (2019) assigned to the University of Bologna.